EBioMedicine 16 (2017) 195–203

Contents lists available at ScienceDirect

EBioMedicine

journal homepage: www.ebiomedicine.com

Research Paper

β1 integrin signaling promotes neuronal migration along vascular scaffolds in the post-stroke brain

Teppei Fujioka [a,b], Naoko Kaneko [a], Itsuki Ajioka [c], Kanako Nakaguchi [a], Taichi Omata [a], Honoka Ohba [a], Reinhard Fässler [d], José Manuel García-Verdugo [e,f], Kiyotoshi Sekiguchi [g], Noriyuki Matsukawa [b], Kazunobu Sawamoto [a,h,*]

[a] Department of Developmental and Regenerative Biology, Nagoya City University Graduate School of Medical Sciences, Nagoya, Aichi 467-8601, Japan
[b] Department of Neurology and Neuroscience, Nagoya City University Graduate School of Medical Sciences, Nagoya, Aichi 467-8601, Japan
[c] Center for Brain Integration Research, Tokyo Medical and Dental University, Bunkyo-ku, Tokyo 113-8510, Japan
[d] Department of Molecular Medicine, Max Planck Institute of Biochemistry, Martinsried 82152, Germany
[e] Laboratory of Comparative Neurobiology, Instituto Cavanilles, Universidad de Valencia, CIBERNED, Valencia 46980, Spain
[f] Multiple Sclerosis and Neural Regeneration Unit, IIS Hospital La Fe, Valencia 46026, Spain
[g] Division of Matrixome Research and Application, Institute for Protein Research, Osaka University, Suita, Osaka 565-0871, Japan
[h] Division of Neural Development and Regeneration, National Institute of Physiological Sciences, Okazaki, Aichi 444-8585, Japan

ARTICLE INFO

Article history:
Received 8 September 2016
Received in revised form 23 December 2016
Accepted 5 January 2017
Available online 9 January 2017

Keywords:
β1 integrin
Laminin
Blood vessel
Chain migration
Vasculature-guided migration
Stroke

ABSTRACT

Cerebral ischemic stroke is a main cause of chronic disability. However, there is currently no effective treatment to promote recovery from stroke-induced neurological symptoms. Recent studies suggest that after stroke, immature neurons, referred to as neuroblasts, generated in a neurogenic niche, the ventricular-subventricular zone, migrate toward the injured area, where they differentiate into mature neurons. Interventions that increase the number of neuroblasts distributed at and around the lesion facilitate neuronal repair in rodent models for ischemic stroke, suggesting that promoting neuroblast migration in the post-stroke brain could improve efficient neuronal regeneration. To move toward the lesion, neuroblasts form chain-like aggregates and migrate along blood vessels, which are thought to increase their migration efficiency. However, the molecular mechanisms regulating these migration processes are largely unknown. Here we studied the role of β1-class integrins, transmembrane receptors for extracellular matrix proteins, in these migrating neuroblasts. We found that the neuroblast chain formation and blood vessel-guided migration critically depend on β1 integrin signaling. β1 integrin facilitated the adhesion of neuroblasts to laminin and the efficient translocation of their soma during migration. Moreover, artificial laminin-containing scaffolds promoted neuroblast chain formation and migration toward the injured area. These data suggest that laminin signaling via β1 integrin supports vasculature-guided neuronal migration to efficiently supply neuroblasts to injured areas. This study also highlights the importance of vascular scaffolds for cell migration in development and regeneration.

1. Introduction

Cerebral ischemic stroke causes marked neuronal loss in the brain, leading to various chronic disabilities in patients. However, there is currently no effective treatment for the neurological symptoms in the post-stroke period.

Recent studies have revealed that neural stem/progenitor cells residing in the ventricular-subventricular zone (V-SVZ) located at the lateral walls of lateral ventricles continuously generate new neurons in the adult mammalian brain (Ihrie and Alvarez-Buylla, 2011). The immature new neurons, referred to as neuroblasts, have a capacity to migrate rapidly in the adult brain tissue toward the olfactory bulb (OB) through a route called the rostral migratory stream (RMS). After a stroke, some of the V-SVZ-derived neuroblasts migrate toward injured areas in the striatum through the complex and dense neuronal and glial network in the mature parenchyma, and differentiate into mature neurons, which are thought to functionally replace damaged neurons and improve neurological deficits (Lindvall and Kokaia, 2015).

For their long-distance migration in brain tissue, neuroblasts use various scaffolds to reach their destination efficiently, where they mature and form neuronal networks. In the developing neocortex, neuroblasts born in the ventricular zone migrate toward the upper layers using radial glial fibers as a scaffold, with which they interact

* Corresponding author at: Department of Developmental and Regenerative Biology, Nagoya City University Graduate School of Medical Sciences, Mizuho-cho, Mizuho-ku, Nagoya 467-8601, Japan.
E-mail address: sawamoto@med.nagoya-cu.ac.jp (K. Sawamoto).

http://dx.doi.org/10.1016/j.ebiom.2017.01.005

through the adhesion molecule N-cadherin (Kawauchi et al., 2010). However, the radial glial fibers disappear within a few weeks of postnatal brain development (Chanas-Sacre et al., 2000). In the adult brain, V-SVZ-derived neuroblasts form elongated chain-like clusters and use neighboring neurons as a scaffold, occasionally contacting blood vessels for long-distance migration in the RMS (Bovetti et al., 2007; Snapyan et al., 2009; Whitman et al., 2009) and in post-stroke striatum toward the injured area (Kojima et al., 2010; Ohab et al., 2006; Yamashita et al., 2006; Zhang et al., 2009).

The vasculature is important for providing a neurogenic niche for stem/progenitor cells and neuroblasts in the V-SVZ under physiological (Shen et al., 2008; Tavazoie et al., 2008; Mirzadeh et al., 2008) and post-stroke (Zhang et al., 2014) conditions. In addition, vascular endothelial cells produce various diffusible signaling molecules that attract and promote the migration of V-SVZ-derived neuroblasts toward a stroke-injured area (Grade et al., 2013; Snapyan et al., 2009; Won et al., 2013). However, the function and molecular basis of the blood vessel-guided neuronal migration are unclear.

β1-class integrins are transmembrane receptors for several extracellular matrix (ECM) proteins, and β1-class integrin-mediated ECM adhesion is involved in the migration of various cell types (Huttenlocher and Horwitz, 2011). The vasculature in the brain is ensheathed by several ECM proteins, including laminin, which is a major ligand for several β1-class integrins (Hallmann et al., 2005). Neuroblasts generated in the adult V-SVZ express β1 integrin, which is necessary for their chain formation during RMS migration (Belvindrah et al., 2007; Emsley and Hagg, 2003; Kokovay et al., 2012). However, how β1 integrin promotes vessel-associated neuronal migration toward injured areas is unknown. Here, using a neuroblast-specific β1 integrin gene knockout mouse line, we show that laminin-β1 integrin signaling enables neuroblasts to form chains and migrate efficiently along blood vessels in the post-stroke brain.

2. Materials and Methods

2.1. Animals

Male 9–12-week-old ICR mice were from SLC (Shizuoka, Japan). *Itgb1*$^{flox/flox}$ mice (Potocnik et al., 2000) were crossed with *nestin-Cre* (Tronche et al., 1999) or *DCX-CreERT2* mice (Stock No. 032780-MU, MMRRC) to obtain *Itgb1* conditional knockouts (*Itgb1*-cKO) and control littermates. *Itgb1*-cKO mice were crossed with *Dcx-DsRed* mice (Wang et al., 2007) or *Rosa26*^{tdTomato} reporter mice (Stock No. 7914, Jackson Laboratory) (Madisen et al., 2010). *Dcx-EGFP* mice were previously described (Gong et al., 2003). All experiments using live animals were performed in accordance with the guidelines and regulations of Nagoya City University.

2.2. Immunohistochemistry

Cell proliferation in the V-SVZ and the migration of neuroblasts were analyzed in 18-day (18d)-post-stroke mice. The animals were deeply anesthetized and perfused transcardially with phosphate buffered saline (PBS, pH 7.4), followed by 4% paraformaldehyde (PFA) in 0.1 M phosphate buffer. Brain sections were prepared and stained as previously described (Kaneko et al., 2010). Briefly, the brain was extracted and post-fixed with the same fixative overnight, then cut into 50-μm-thick coronal sections on a vibratome (VT1200S, Leica, Wetzlar, Germany). The sections were incubated for 1 h in blocking solution (10% donkey serum and 0.4% Triton X-100 in PBS), overnight at 4 °C with primary antibodies, and 2 h at room temperature with Alexa Fluor-conjugated secondary antibodies (1:1000, Invitrogen, MA, USA). Signals were amplified with biotinylated secondary antibodies (1:1000, Jackson Laboratory, West Grove, PA, USA) and the Vectastain Elite ABC kit (Vector Laboratories, Burlingame, CA, USA), and visualized using the TSA Fluorescence System (PerkinElmer, Waltham, MA, USA). For Ki67 staining, the sections were pretreated with 1% H_2O_2 for 40 min before blocking. The following primary antibodies were used: goat anti-DCX (1:100, Santa Cruz Biotechnology, Dallas, TX, USA), mouse anti-GFAP (1:500, Sigma-Aldrich, St. Louis, MO, USA), chick anti-laminin (1:200, Abcam, Cambridge, UK), rat anti-β1 integrin (1:100, Merck Millipore, Billerica, MA, USA), rat anti-CD29, clone 9EG7 (1:100, BD Biosciences, Franklin Lakes, NJ, USA), rat CD31 (1:100, BD Biosciences), rat anti-BrdU (Abcam), rabbit anti-DsRed (1:200, Clontech, Mountain View, CA, USA), rat anti-GFP (1:100, Nacalai, Kyoto, Japan), rabbit anti-Iba1 (1:2000, Wako Pure Chemical Industries, Osaka, Japan), mouse anti-calretinin (1:3000, Millipore), mouse anti-NeuN (1:100, Millipore), and rabbit anti-Ki67 (1:200, Leica). Cellular nuclei were stained with Hoechst (1:5000, Invitrogen). For quantification using post-stroke brains, coronal sections through the V-SVZ were used. For the quantification of migrating neuroblasts in the RMS, coronal brain sections throughout the RMS and the OB were used. To visualize and count double-labeled cells, confocal z-stack images were captured using a confocal laser microscope (LSM700, Carl Zeiss, Jena, TH, Germany) with a 20×/0.8 or 40×/1.2 objective lens. In the histological analyses, the actual number of cells in every other or third 50-μm-thick coronal section was bilaterally counted, and the number was multiplied by two or three, respectively, to obtain the total number of cells per brain.

2.3. Induction of Ischemic Stroke

Mice were anesthetized with an oxygen/N_2O/isoflurane mixture (65.3/32.7/2.0%) administered through an inhalation mask and placed on a 37 °C heating bed (model BMT-100, Bio Research Center, Nagoya, Japan). Middle cerebral artery occlusion was induced by the intraluminal filament technique, as reported previously (Hara et al., 1996) with several modifications. In brief, after occlusion of the common carotid artery, the right carotid bifurcation was exposed, and the external carotid artery was coagulated distal to the bifurcation. A 10.0-mm silicone-coated 8-0 filament was then inserted through the stump of the external cerebral artery and gently advanced to occlude the middle cerebral artery, and the incision was closed. The mice were re-anesthetized 50–60 min later, the incision was re-opened, and the filament was gently withdrawn. The incision was then closed again. This procedure minimized the total time the mouse was under anesthesia.

2.4. BrdU Injection

To label proliferating cells, bromodeoxyuridine (BrdU, Sigma-Aldrich, 50 mg/kg, dissolved in PBS) was injected into mice intraperitoneally, as described in each figure and legend.

2.5. Tamoxifen Injection

Tamoxifen (Sigma-Aldrich) was dissolved in solvent (20 mg/ml tamoxifen, 90% sesame oil, 6% ethanol, 4% DMSO). For stroke experiments, *Itgb1*-cKO (*Itgb1*$^{flox/flox}$*;DCX-CreERT2;Rosa26*$^{tdTomato/tdTomato}$) and control (*DCX-CreERT2;Rosa26*$^{tdTomato/tdTomato}$) mice were treated with tamoxifen at 13 and 15 d-post-stroke intraperitoneally (300 μg/g), which caused the deletion of β1 integrin specifically in neuroblasts. For the analysis of neuroblast migration in the RMS in intact mice, *Itgb1*-cKO (*Itgb1*$^{flox/flox}$*; DCX-CreERT2*) and control (*Itgb1*$^{flox/flox}$) mice were treated with tamoxifen twice, 48 h apart, prior to BrdU treatment.

2.6. Electron Microscopy

Animals were deeply anesthetized and perfused transcardially with 20 ml of PBS (pH 7.4) followed by 50 ml of 2% PFA-2.5% glutaraldehyde (GA) in 0.1 M phosphate buffer. The brain was extracted, post-fixed with the same fixative overnight, and cut into 200-μm coronal sections on a vibratome (VT1200S, Leica). The sections were post-fixed with 1% OsO_4 in 0.1 M phosphate buffer for 2 h, block-stained in 2% uranyl

acetate, dehydrated with a graded series of alcohol, and embedded in Araldite (Durcupan, Fluka Biochemika, Ronkonkoma, NY). Serial semi-thin sections (2.0-μm-thick) were cut with an ultramicrotome (UC6, Leica), and stained lightly with 1% toluidine blue. Subsequently, selected levels were glued to Durcupan blocks and detached from the glass slide by repeated freezing in liquid nitrogen and thawing. From the semi-thin sections, ultra-thin sections (60–70 nm-thickness) were prepared using an ultramicrotome, and stained with lead citrate (Reynolds' solution). Photomicrographs were obtained under a JEM1011J transmission electron microscope (JEOL, Tokyo, Japan) using a digital camera.

Photomicrographs showing the cellular contact among chain of neuroblasts, astrocytes, and blood vessels in the striatum of control (*DCX-CreERT2;Rosa26*$^{tdTomato/tdTomato}$) and *Itgb1*-cKO (*Itgb1*$^{flox/flox}$*;DCX-CreERT2;Rosa26*$^{tdTomato/tdTomato}$) mouse were taken at a magnification of ×50,000. The length of junction between neuroblasts in the control and *Itgb1*-cKO mouse were quantified using ImageJ software (National Institutes of Health). Neuroblasts were identified by their very electron-dense nucleus and cytoplasm, whereas astrocytes were identified by their electron-lucent nucleus and cytoplasm and the presence of intermediate filaments and glycogen granules, as previously described (Doetsch et al., 1997).

2.7. Time-lapse Imaging of Post-stroke Brain Slices

Brain slices were prepared for time-lapse imaging from adult *Itgb1*-cKO mice (*Itgb1*$^{flox/flox}$*;DCX-CreERT2;Rosa26*$^{tdTomato/tdTomato}$) or control mice (*DCX-CreERT2;Rosa26*$^{tdTomato/tdTomato}$) at 16–18 d-post-stroke, as reported previously (Grade et al., 2013), with modifications. Briefly, blood vessels were labeled by cardiac perfusion with 10 ml of fluorescent ink (×50, spotliter Cream yellow, PILOT, Tokyo, Japan) diluted in PBS, as reported previously (Li et al., 2008; Takase et al., 2013). The brain was dissected and cut into coronal slices (170-μm thick) using a vibratome (VT1200S, Leica). The slices were placed on a stage-top imaging chamber (Warner Instruments, Hamden, CT, USA) under continuous perfusion with artificial cerebrospinal fluid (aCSF, 1 ml/min, containing 125 mM NaCl, 26 mM $NaHCO_3$, 3 mM KCl, 2 mM $CaCl_2$, 1.3 mM $MgCl_2$, 1.25 mM NaH_2PO_4, and 20 mM Glucose, pH 7.4, maintained at 38 °C, bubbled with 95% O_2 and 5% CO_2) during the imaging. Using a confocal laser microscope (LSM710, Carl Zeiss) equipped with a gallium arsenide phosphide detector, z-stack images (4–11 z-sections with 3–5-μm step sizes) were captured every 5–15 min for 8–16 h. To quantify the speed of neuroblast migration along blood vessels in the captured images, neuroblasts in the striatum with a monopolar or bipolar shape were traced using ImageJ software (manual tracking plugin). Only the neuroblasts that could be continuously tracked for at least 90 min were used for this analysis. We defined cells in the 'resting phase' as those in which the soma moved slower than 6 μm/h.

2.8. Culture of V-SVZ-derived Neuroblasts in Collagen Gel

Collagen gel experiments were performed as described previously (Wichterle et al., 1997) with several modifications. In brief, Glass-bottom 35-mm Petri dishes were coated with poly-L-lysine (PLL: Sigma-Aldrich, 0.1 μg/cm^2, incubated 2 h) or PLL and laminin-111 (Wako, 2.6 μg/cm^2, incubated overnight). For time-lapse imaging, the V-SVZ was dissected from P2–6 *Itgb1*-cKO (*Itgb1*$^{flox/flox}$*;nestin-Cre;Dcx-DsRed*) mice or control littermates, cut into 150–200-μm-diameter pieces, mixed with collagen (PureCol, Bovine collagen solution type 1, Advanced Biomatrix, San Diego, CA, USA, diluted to 2.7 mg/ml in PBS), and applied to the PLL/laminin-coated dishes. The dishes were maintained in a humidified, 5% CO_2, 37 °C incubator to allow the explant mixture to congeal on the dishes. The gel containing the explant was overlaid with 2 ml of serum-free Neurobasal medium (Invitrogen) containing 2% B27 (Invitrogen), 50 U/ml penicillin-streptomycin, and 2 mM L-glutamine, and then cultured in the incubator for 24 h before imaging. Time-lapse video recordings were obtained using an inverted light microscope (Axio-Observer, Carl Zeiss) equipped with the Colibri light-emitting diode light system, using a ×20 (Fig. 3a, Movie S3, S5, S6) and ×40 (Fig. 3d, Movie S4) dry objective lens. Every 5 min (Fig. 3a, Movie S3, S5, S6) or 1 min (Fig. 3d, Movie S4), z-stack images (1–5 z-sections with 3–5-μm step sizes) were obtained automatically for 8–12 h. The migration speeds of the soma and growth cone were quantified using ImageJ software. The time of adhesion to the bottom of the dish was calculated manually from the z-stack images. We defined cells in the 'resting phase' as those in which the soma moved slower than 30 μm/h.

2.9. Laminin-containing Porous Sponge

We previously designed a laminin-rich porous sponge (Laminin sponge) based on the components and morphology of blood vessel scaffolds (Ajioka et al., 2015). The laminin sponge or control sponge was placed near V-SVZ explants dissected from P2–6 *Itgb1*-cKO mice or control littermates in collagen gel. The migration behavior of neuroblasts migrating in contact or not in contact with the sponge was recorded as described above.

2.10. Injection of Laminin-rich Biomaterial

To assess whether an artificial structure containing laminin promotes neuronal migration, we used an injectable self-assembling scaffold that forms through the spontaneous assembly of ionic self-complementary β-sheet oligopeptides under physiological conditions (Holmes et al., 2000). A synthetic peptide hydrogel (PuraMatrix, Corning, NY, USA, 1.0% w/v) was mixed with the same volume of laminin solution (1.0 μg/μl) following the manufacture's protocol, and then stereotaxically injected into the ipsilateral medial striatum (1 μl/mouse, relative to bregma: anterior, 1.7 mm; depth, 4.0–3.0 mm, rotated axially by 45°) of intact or 10 d-post-stroke mice. To visualize laminin, 200 μg of laminin was reacted with 50 μg/ml DyLight 650 NHS Ester (Pierce Biotechnology, IL, USA) in PBS for 1 h. To examine the responses of glial cells to hydrogels in the intact brain (Fig. S3), or the migration of V-SVZ-derived cells along the laminin scaffold in the post-stroke brain (Fig. 4c–f), the brain was fixed 8 d later (18 d-post-stroke). To examine the maturation of neuroblasts in the post-stroke striatum, the brain was fixed 18 d later (28 d-post-stroke) (Fig. S4).

2.11. Coculture of V-SVZ-derived Neuroblasts With Striatal Astrocytes

The striatum or the V-SVZ was dissected from P3–7 WT mice in L-15 medium (Invitrogen) and dissociated with trypsin-EDTA (Invitrogen). The dissociated cells were washed with L-15 medium, plated, and cultured in DMEM containing 10% FBS, 50 U/ml penicillin-streptomycin, and 2 mM L-glutamine. To purify astrocytes from the mixed culture, the cells were incubated with shaking for 60 min before the first passage. The cells were dissociated from the dishes using trypsin-EDTA (Invitrogen), re-plated, and cultured at confluent density. The V-SVZ dissected from *Itgb1*-cKO mice or control littermates was plated on the monolayer culture of astrocytes in serum-free Neurobasal medium containing 2% B27, 50 U/ml penicillin-streptomycin, and 2 mM L-glutamine, and cultured in an incubator (5% CO_2, 37 °C) for 12 h before imaging. The migration behavior of neuroblasts on the astrocyte monolayer was recorded as described above.

2.12. Transplantation of V-SVZ Cells

For transplantation experiments, the V-SVZ of P1–6 *Dcx-EGFP* or *nestin-Cre;Itgb1*$^{flox/flox}$*;Dcx-DsRed* mice was dissected and dissociated using trypsin-EDTA (Invitrogen) as previously described (Kaneko et al., 2010). The cell suspension (3 μl) was stereotaxically injected into

the V-SVZ (relative to bregma: anterior, 1.1 mm; lateral, 1.05 mm; depth, 2.8–2.0 mm) of wild-type mice, then fixed 5 d later.

2.13. Statistics

All data were expressed as the mean ± standard error of the mean (SEM). Differences between means were determined by two-tailed Student's *t*-test, paired *t*-test, or one-way ANOVA followed by Tukey-Kramer multiple comparison test or Dunnett's multiple comparison test, unless otherwise specified. A p-value < 0.05 was considered statistically significant.

3. Results

3.1. β1 integrin Is Expressed in V-SVZ-derived Chain-forming Neuroblasts Associated With Blood Vessels

We first analyzed the β1 integrin expression in the migrating neuroblasts in intact (Fig. 1a–b) and post-stroke (Fig. 1c–h) adult mouse brains by immunohistochemistry. In the intact brain, almost all of the doublecortin (DCX)-positive (+) neuroblasts in the V-SVZ and RMS expressed β1 integrin (Fig. 1b), as previously reported (Belvindrah et al., 2007; Emsley and Hagg, 2003). After reaching the

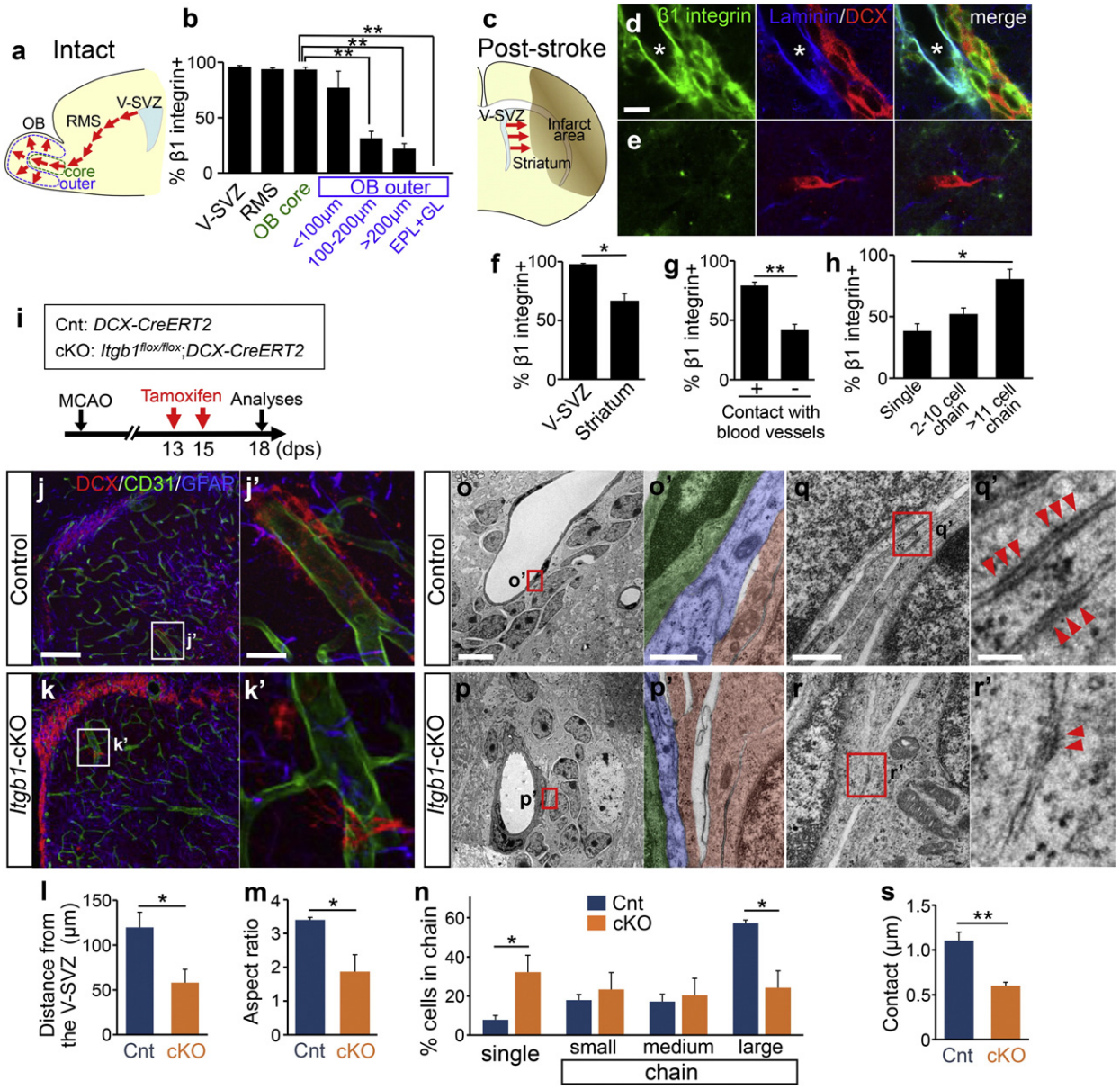

Fig. 1. Role of β1 integrin in neuroblast chain formation and efficient migration toward an injured site. a: Schema of an adult mouse sagittal brain section showing the migration route of neuroblasts (red arrows). V-SVZ: ventricular-subventricular zone, RMS: rostral migratory stream, OB: olfactory bulb. b: Percentage of DCX+ neuroblasts that were β1 integrin+ in each part of the migration route. EPL: external plexiform layer, GL: glomerular layer. c: Schema of a coronal section of post-stroke mouse brain showing the migration route of neuroblasts toward the injured area (red arrows). d–e: Section of 18 d-post-stroke brain immunostained for β1 integrin (green), DCX (red), and laminin (blue) (asterisks: a blood vessel). f–h: Percentage DCX+ cells that were β1 integrin+ in the striatum or V-SVZ (f), with or without blood-vessel contact (g), and migrating individually or in chains of various sizes (h). i: Experimental design. dps: days-post-stroke. j–k: Post-stroke brain sections stained for DCX (red), CD31 (green), and GFAP (blue). l–m: Mean migration distance of neuroblasts from the V-SVZ (l), aspect ratio of the neuronal chains (m), and percentage of neuroblasts integrated into small (2–5 cells), medium (6–9 cells), or large (>10 cells) chains (n) in the post-stroke striatum. o–s: Electron microscopy. Chains of neuroblasts (red) in the post-stroke striatum in contact with astrocytes (blue) and blood vessels (green) (o–p'), and adherent-like junctions between neuroblasts (q–r', arrowheads). Mean junction length in the Cnt and cKO groups is shown in (s). Data are the mean ± SEM; b, f–h: $n = 4$ mice, l–n: $n = 6$ mice (Cnt), $n = 8$ mice (cKO); $^{*}p < 0.05$, $^{**}p < 0.01$. Scale bars, 50 μm: j, 20 μm: j', 10 μm: d, 5 μm: o, 0.5 μm: o', q, 0.1 μm: q'.

OB, neuroblasts detached from the chains and individually migrated toward the outer layers, i.e., the external plexiform layer (EPL) and glomerular layer (GL), where the proportion of β1 integrin-expressing neuroblasts was lower than in the OB core (Fig. 1a–b).

In the post-stroke brain, V-SVZ-derived neuroblasts frequently migrated toward the injured area along blood vessels that were enwrapped in laminin, a major ligand for β1 integrin (Fig. 1c–d). We thus examined the β1 integrin expression in DCX+ neuroblasts migrating toward the infarct area in the striatum 18 days (18 d)-post-stroke. Although the proportion of β1 integrin+ neuroblasts (DCX+ cells with moderate to high levels of β1 integrin immunoreactivity) migrating in the striatum was lower than in the V-SVZ (Fig. 1f), it was greater for neuroblasts in contact with blood vessels than for those not in contact (Fig. 1d–e, g). The proportion of β1 integrin+ cells was also greater in DCX+ cells integrated into large chains containing > 11 cells than in those migrating individually (Fig. 1h). These findings suggest that β1 integrin in neuroblasts might be involved in their blood vessel-associated chain migration in the post-stroke brain.

3.2. β1 Integrin Is Required for Efficient Neuroblast Migration Toward Injured Areas

In the adult brain, in addition to migrating neuroblasts, β1-class integrins are expressed in astrocytes, pericytes, and vascular endothelial cells, which form blood vessels (Wu and Reddy, 2012). To investigate β1 integrin's role specifically in neuroblasts in the injured striatum, we generated a new mouse line (*Itgb1*-cKO: *Itgb1*$^{flox/flox}$;*DCX-CreERT2*), in which tamoxifen treatment induces a Cre recombinase-dependent *Itgb1* gene deletion in neuroblasts. The *Itgb1*-cKO mice were treated with tamoxifen at 13 d- and 15 d-post-stroke, and the neuroblasts in the injured striatum were examined at 18 d-post-stroke (Fig. 1i–s). Although the neuroblast-specific *Itgb1* deletion did not affect the number of Ki67+ cells in the V-SVZ (data not shown), the number of migrating neuroblasts in the ipsilateral striatum (Cnt: 685 ± 92, cKO: 329 ± 64, $p = 0.0067$, mean ± SEM) and their mean migration distance from the V-SVZ were smaller in the cKO than in the control (Cnt: *DCX-CreERT2*) group (Fig. 1l). On the other hand, there was no significant difference in the neuroblasts' migration capacity in the V-SVZ-RMS-OB pathway between these groups (Fig. S1), suggesting that the dependency on β1 integrin is greater for neuroblasts migrating toward the injured site than for those in the RMS. In the post-stroke striatum, unlike the elongated morphology of the chain-forming neuroblasts observed along blood vessels in the Cnt group (Fig. 1j), the cKO neuroblasts formed globular aggregates (Fig. 1k, m). In the cKO mice, a larger proportion of neuroblasts migrated individually, and fewer formed large aggregates of >10 cells compared with the Cnt group (Fig. 1n). Electron microscopy revealed that the length of adherent-like junction between neuroblasts was smaller in the cKO group (Fig. 1o–s). These results suggested that β1 integrin on the neuroblasts regulates their interaction with each other to form chains and their interaction with blood vessels to facilitate their migration toward an injury.

We next compared the migration behavior of the Cnt and cKO neuroblasts along vascular scaffolds using time-lapse imaging of 18 d-post-stroke brain slices. To visualize neuroblasts, these mouse lines were crossed with *Rosa26*^{tdTomato} reporter mice (Madisen et al., 2010). Blood vessels were labeled by cardiac perfusion with fluorescent ink (Takase et al., 2013). Chain migration along the vessels was frequently observed in Cnt mice, but rarely in cKO mice (Movie S1). As it was difficult to examine the behavior of each cell in an aggregate, we studied the behavior of individually migrating neuroblasts along the labeled blood vessels. These cells extended a leading process along the vessel and showed a typical saltatory movement of the soma (Schaar and McConnell, 2005) (Fig. 2a, Movie S2). The average speed of these neuroblasts was slower in the cKO group than in the Cnt group (Fig. 2b), suggesting that β1 integrin accelerates vessel-associated neuronal migration in the injured striatum. Together, these results suggest that neuroblasts require β1 integrin for association and spreading on and efficient migration along vascular scaffolds toward injured sites in the post-stroke brain.

3.3. Migrating Neuroblasts Require β1 Integrin for Laminin-dependent Adhesion and Somal Translocation

To examine how β1 integrin promotes neuronal migration, we performed time-lapse imaging of *Itgb1*-cKO (*Itgb1*$^{flox/flox}$;*nestin-Cre*) neuroblasts migrating on a laminin-coated glass surface embedded in collagen gel. Cnt neuroblasts formed chain-like elongated aggregates when they migrated on laminin-coated surface, but not when they migrated on a PLL-coated glass surface (Fig. 3a, Movie S3). In contrast, cKO neuroblasts failed to assemble chain-like structures on laminin-coated surface. Furthermore, Cnt neuroblasts spent a longer time in contact with the laminin-coated surface (Fig. 3b) and migrated faster (Fig. 3c) compared with cKO cells or Cnt cells on the PLL-coated surface (Movie S4). The analysis of individually migrating neuroblasts (Fig. 3d–h) revealed that Cnt neuroblasts attached to the laminin-coated surface showed rapid and saltatory movements on the laminin-coated surface, in which somal translocation immediately followed the leading process extension (Fig. 3d–e). In sharp contrast cKO neuroblasts, although extending the leading process with normal speed (Fig. 3g), displayed a disturbed somal translocation with increased resting (Fig. 3f) and swelling (Fig. 3h) periods, similarly as observed in brain slices (Fig. 2c).

Electron microscopy revealed that neuroblasts migrating along blood vessels in the post-stroke brain did not directly contact the vascular endothelial cells, but did contact astrocytic processes enwrapping the vessels (Fig. 1o') (Yamashita et al., 2006; Kojima et al., 2010). These astrocytes express laminin as do endothelial cells (Fig. S2), as previously reported (Sixt et al., 2001). Therefore, we analyzed β1 integrin's role in the interaction between migrating neuroblasts and striatal astrocytes (Fig. 3i–k). Time-lapse imaging showed that neuroblasts migrating on a monolayer of astrocytes dissociated from the striatum frequently assembled into chain-like aggregates in the Cnt, but not in the cKO group (Movie S5). The speed and efficiency ratio (straight-line distance between the start and end points divided by the total migratory distance of each cell) of individually migrating neuroblasts were decreased in the cKO group (Fig. 3j–k). These results suggest that neuroblasts require β1 integrin to adhere stably to laminin-rich structures for their efficient somal translocation.

3.4. Laminin-containing Artificial Scaffolds Promote Neuronal Migration

We next examined whether laminin-rich blood vessel-like structures could promote neuroblast migration. V-SVZ neuroblasts were cultured with laminin-containing (laminin-) or -non-containing (Cnt-) porous sponge (Ajioka et al., 2015) embedded in collagen gel, and the migration speed of neuroblasts with or without contact with the sponge surface was quantified by time-lapse imaging. Both Cnt and *Itgb1*-cKO neuroblasts labeled with DsRed were distributed close to the laminin- and Cnt-sponges (Fig. 4a and data not shown). There was no significant difference in speed between Cnt and *Itgb1*-cKO neuroblasts when they migrated apart from the sponges, consistent with the observation that *Itgb1*-cKO and Cnt neuroblasts showed similar migration speeds on a culture dish surface coated without laminin (Fig. 3b–c). However, when migration occurred along a sponge surface, Cnt neuroblasts on a laminin-sponge migrated faster than cKO neuroblasts on a laminin-sponge and Cnt neuroblasts on a Cnt-sponge (Fig. 4b, Movie S6). These data suggest that a laminin-rich scaffold accelerates the migration of neuroblasts via β1 integrin.

Finally, we tested whether an artificial laminin scaffold could promote neuronal migration in the post-stroke brain. An injectable hydrogel with or without laminin (Laminin- and Cnt-hydrogel, respectively), which self-assembles from a soluble state into hydrated nanofibers *in vivo* (Holmes et al., 2000), was injected into the striatum of 10 d-post-

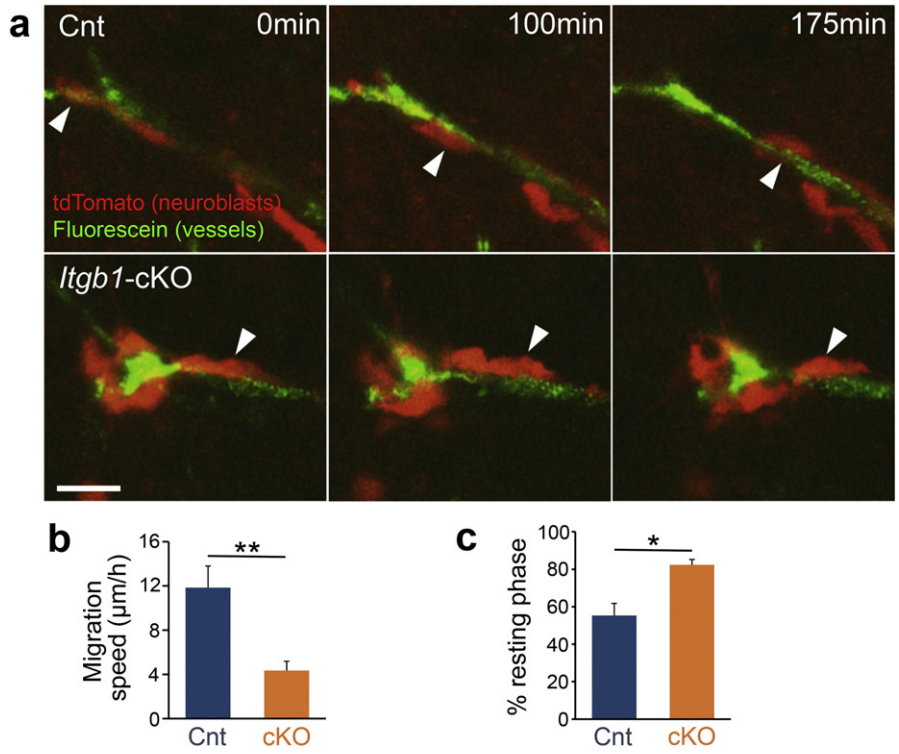

Fig. 2. Effects of neuroblast-specific β1 integrin deletion on blood vessel-associated neuronal migration in cultured post-stroke brain slices. Time-lapse images of tdTomato-labeled (red) migrating neuroblasts (arrowheads) associated with blood vessels (green) in post-stroke control (Cnt) and *Itgb1*-cKO brain slices (a). Mean speed (b) and percent resting-phase duration (c) in the neuroblasts migrating along blood vessels. Data are the mean ± SEM; $n = 15$ cells from 11 mice (Cnt), $n = 17$ cells from 12 mice (cKO); $^{*}p < 0.05$, $^{**}p < 0.01$, Scale bar, 20 μm.

stroke brains (Fig. 4c). The migration of DCX+ neuroblasts along the hydrogel toward the injured area was examined 8 days later. More migrating neuroblasts were observed on the laminin-hydrogel than on the Cnt-hydrogel, and they only formed chains in the Laminin-hydrogel group (Fig. 4d–f), suggesting that the artificial laminin scaffold can efficiently mimic the vasculature and facilitate neuronal migration toward the injured area. On the other hand, there was no significant difference in the number of GFAP+ astrocytes or Iba1+ microglia in the striatum at and around the injection site between the groups (Fig. S3). Taken together, we conclude that β1 integrin expressed in the V-SVZ neuroblasts promotes their efficient chain migration along laminin-containing scaffolds toward the injured area in the post-stroke brain.

4. Discussion

In addition to the migration of V-SVZ-derived neuroblasts toward the injured site in the post-stroke brain, as we and others have previously reported (Kojima et al., 2010; Ohab et al., 2006; Yamashita et al., 2006), vasculature-guided migration occurs in various tissues and situations, such as in lymphatic endothelial cells and oligodendrocyte precursors during development (Bussmann et al., 2010; Tsai et al., 2016), Schwann cells in peripheral nerve regeneration (Cattin et al., 2015), and tumor cells in the brain (Farin et al., 2006; Lugassy and Barnhill, 2007). However, the molecular mechanisms for these cells' adhesion to and migration along blood vessels are unknown. Here we demonstrated that neuroblast-expressed β1-class integrins, receptor proteins that form heterodimers with multiple α subunits to bind various ECM proteins, are required for the neuroblasts' blood vessel-guided migration. We found that deleting β1 integrin specifically in neuroblasts affected their morphology and migration speed on laminin-coated materials, suggesting that the laminin on blood vessels functions as a ligand to control the migration of β1 integrin-expressing neuroblasts. In future studies, it will be important to examine whether the integrin-mediated mechanism we discovered in V-SVZ-derived neuroblasts also acts in other cells as a general regulator of vasculature-guided migration.

V-SVZ-derived neuroblasts exhibit saltatory movement, with alternating resting and migratory phases (Wichterle et al., 1997). In the resting phase, a leading process is extended, and centrosome and Golgi apparatus move into it (swelling phase), followed by nuclear translocation and detachment of the rear (migratory phase) (Schaar and McConnell, 2005). During migration on a laminin-coated dish, β1 integrin gene deletion still allowed the leading process extension and swelling to proceed normally, but impaired the stable attachment of neuroblasts to the substrate and the initiation/promotion of nuclear translocation, leading to an increased resting phase and decreased migration speed (Fig. 3). Similar defects were observed in β1 integrin-deficient neuroblasts migrating along blood vessels in living brain slices (Fig. 2). These findings suggest that the stable attachment of neurons to a laminin-containing scaffold mediated by neuronal β1 integrin facilitates the somal translocation processes such as anterior movement of the nucleus and actomyosin-mediated contraction of the rear.

The V-SVZ-derived neuroblasts migrating along blood vessels assemble into chains similar to those in the RMS (Yamashita et al., 2006). The deletion of β1 integrin or laminin from neural cells impairs the chain formation in the RMS (Belvindrah et al., 2007; Emsley and Hagg, 2003). Our electron microscopy showed that β1 integrin on the neuroblasts was required for the formation of appropriate interneuronal adhesions (Fig. 1). *In vitro* chain assembly of neuroblasts occurred only when they attached to a laminin-rich substrate, a laminin-containing sponge fiber, or an astrocytic monolayer, in a β1 integrin-dependent manner (Figs 2, 3, and 4). Neuroblasts migrating along blood vessels contact astrocytic processes surrounding the vascular basal lamina rather than endothelial cells (Kojima et al., 2010; Yamashita et al., 2006; this work). These results suggest that laminin-β1 integrin signaling directly causes cytoskeletal reorganization in neuroblasts (Huttenlocher and Horwitz, 2011) and/or the assembly of other cell-adhesion molecules such as cadherins (Mui et al., 2016) to promote chain migration.

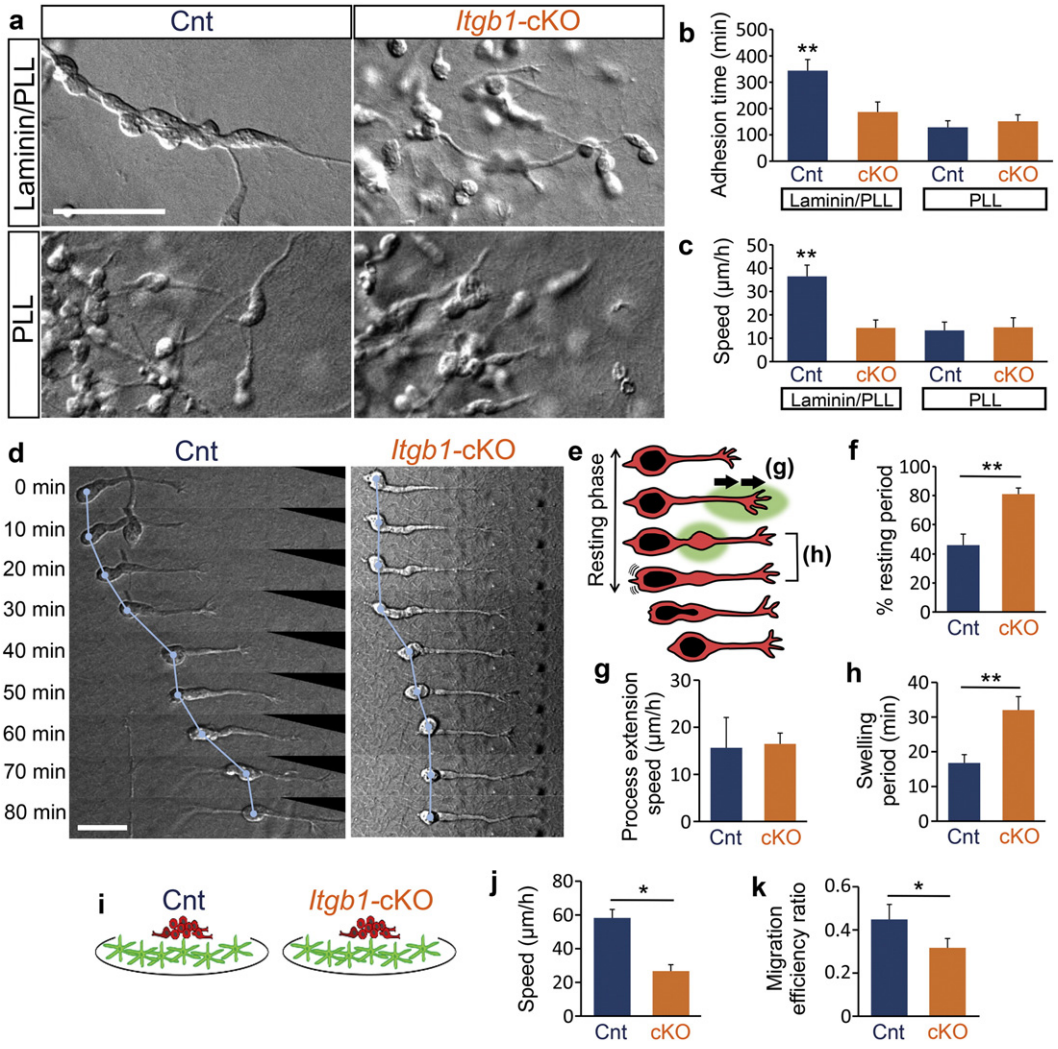

Fig. 3. Laminin-β1-integrin-mediated adhesion promotes neuroblast chain formation and migration. a: Phase-contrast images of control (Cnt) and *Itgb1*-cKO (cKO) neuroblasts migrating on a culture dish surface coated with or without laminin. See also Movie S3. b–c: Duration of adhesion with the dish surface (b) and speed (c) of migrating neurons. d–h: Saltatory movement of neuroblasts. Time-lapse imaging of Cnt and cKO neuroblasts migrating in contact with a laminin-coated dish surface (d, see Movie S4). Schema of saltatory neuronal migration (e), percentage of resting period (f), speed of the extending leading tip (g), and duration of swelling period (h). i–k: Migration of Cnt and cKO neuroblasts cultured on a monolayer of striatal astrocytes (i). Neuroblast migration speed (j) and efficiency (k). Data are the mean ± SEM; b–c: $n = 18$–20 cells, f–h: $n = 7$ cells, j–k: $n = 11$–20 cells, at least two independent experiments; $^{*}p < 0.05$, $^{**}p < 0.01$. Scale bars, 50 μm: a, 20 μm: d.

Furthermore, restricting the anchoring of neuroblasts onto the vascular surface probably increases the chance for them to contact each other and align along the scaffold. Indeed, this feature can be exploited by allowing the β1 integrin-expressing neuroblasts to migrate along an artificial laminin-rich scaffold, which promotes their chain formation and efficient migration toward the injured area in the post-stroke striatum.

Although the extent of post-stoke neurogenesis in the human brain is still unclear, post-mortem brain studies have shown an increase in cell proliferation in the V-SVZ (Macas et al., 2006; Minger et al., 2007; Marti-Fabregas et al., 2010) and an emergence of neural progenitor cells and/or neuroblasts in the peri-infarct area (Jin et al., 2006, Minger et al., 2007), which are closely associated with blood vessels (Jin et al., 2006). These observations suggest that the neurogenic response of the V-SVZ and the blood vessel-guided migration of neuroblasts toward the injured site in the post-stroke brain may be evolutionarily conserved, even in humans. Although agents that block integrin signaling have been clinically applied to inhibit the invasion of cancer cells or the migration of immune cells (Ley et al., 2016), therapeutic interventions that increase integrin signaling to promote cellular migration have not been reported. We previously reported that neuroblasts migrate into laminin-rich porous sponge transplanted into the injured cortex of neonatal mice (Ajioka et al., 2015). Here we have demonstrated the effects of an injectable self-assembling laminin-rich scaffold, which is less invasive and more applicable for clinical use, in adult animals. The migration of V-SVZ neuroblasts into the post-stroke striatum was significantly promoted by the laminin-rich hydrogel, although only small numbers of newly generated mature neurons were observed in the striatum 4 weeks after stroke (Fig. S4). In combination with additional treatments that promote the survival and neuronal differentiation of V-SVZ-derived neuroblasts in the post-stroke brain, artificial scaffolds containing ECM proteins to promote cell migration may become a useful intervention for regenerating brain tissue.

Supplementary data to this article can be found online at http://dx.doi.org/10.1016/j.ebiom.2017.01.005.

Founding Sources

This work was supported by research grants from JSPS [Kakenhi 26250019 and 22122004, NEXT program (LS104), Bilateral Open Partnership Joint Research Projects to K.Sa., Program for Advancing Strategic International Networks to Accelerate the Circulation of Talented Researchers (S2704) to K.Sa. and JMG-V, Takeda Science Foundation (to K.Sa.), Terumo Foundation for Life Sciences and Arts (to K.Sa. and I.A.) and Grant-in-Aid for Research at Nagoya City University (to K.Sa.)].

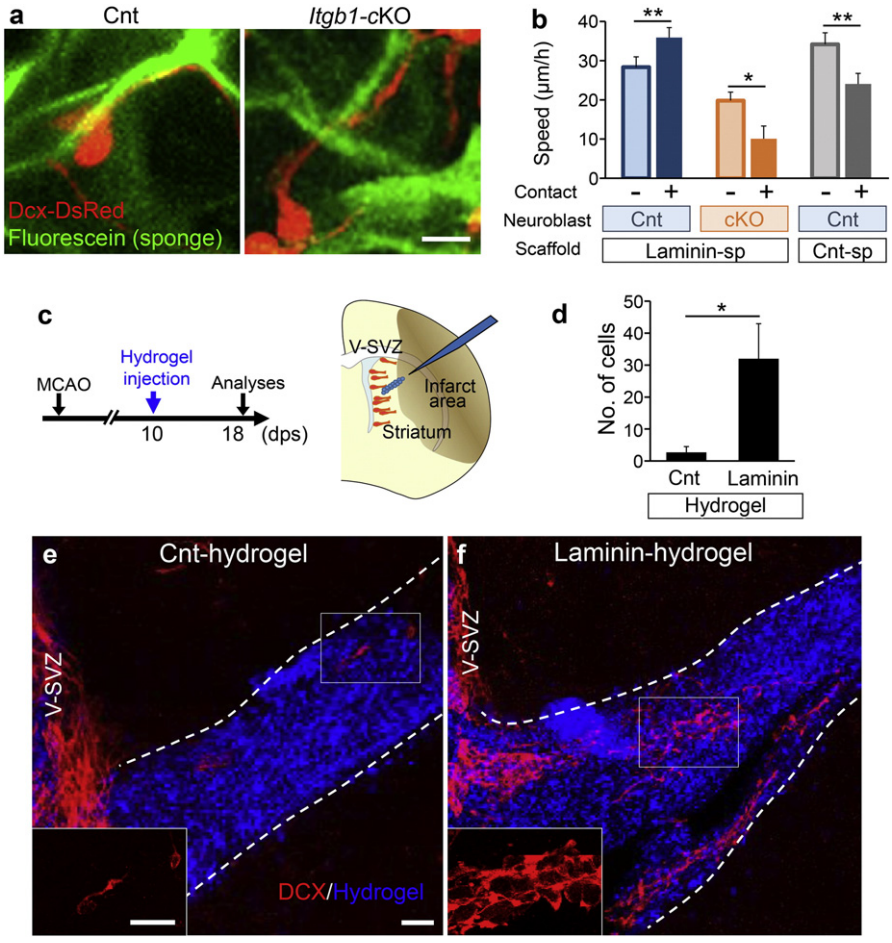

Fig. 4. Laminin scaffolds promote neuronal migration via β1 integrin. a–b: Migration of neuroblasts in contact with the sponge surface. DsRed-labeled control (Cnt) or *Itgb1*-cKO (cKO) neuroblasts embedded in collagen gels with fluorescein-labeled porous gelatin sponge containing (laminin-sp) or not containing (Cnt-sp) laminin. Both Cnt and cKO neuroblasts (red) contacted the laminin-sp. surface (green) (a). Migration speed of neuroblasts with or without sponge contact (b). c–f: Migration of neuroblasts along an artificial laminin scaffold toward an injured area. Experimental procedure (c). Number (d) and confocal images (e–f) of neuroblasts (red) migrating along the fluorescently labeled hydrogel (blue) without and with laminin in coronal sections of the post-stroke striatum. Insets show higher magnification images of the boxed area. Data are the mean ± SEM; b: $n = 9$–22 cells, 3 independent experiments, d: $n = 7$ mice; $^{*}p < 0.05$, $^{**}p < 0.01$. Scale bars, 20 μm: e, 10 μm: a.

Author Contributions

T.F., N.K., I.A., K.N., T.O, and H.O. performed experiments and collected data. T.F., N.K., I.A., R.F., J.M.G-V., K.Se, N.M and K.Sa designed the study and/or interpreted the data. T.F., N.K., and K.Sa wrote the manuscript.

Conflict of Interest Statement

All the authors declare no conflict of interest.

Acknowledgements

We thank Dr. M. Yamaguchi for the *Rosa26*^{tdTomato} reporter mice, Drs. T. Shinohara and S. Takashima for the *Itgb1*$^{flox/flox}$ mice, the Mutant Mouse Regional Resource Center (MMRRC) for the *DCX-CreERT2* mice, and Drs. I. Miyoshi and A. Saghatelyan for technical support.

References

Ajioka, I., Jinnou, H., Okada, K., Sawada, M., Saitoh, S., Sawamoto, K., 2015. Enhancement of neuroblast migration into the injured cerebral cortex using laminin-containing porous sponge. Tissue Eng. A 21, 193–201.

Belvindrah, R., Hankel, S., Walker, J., Patton, B.L., Muller, U., 2007. Beta1 integrins control the formation of cell chains in the adult rostral migratory stream. J. Neurosci. 27, 2704–2717.

Bovetti, S., Hsieh, Y.C., Bovolin, P., Perroteau, I., Kazunori, T., Puche, A.C., 2007. Blood vessels form a scaffold for neuroblast migration in the adult olfactory bulb. J. Neurosci. 27, 5976–5980.

Bussmann, J., Bos, F.L., Urasaki, A., Kawakami, K., Duckers, H.J., Schulte-Merker, S., 2010. Arteries provide essential guidance cues for lymphatic endothelial cells in the zebrafish trunk. Development 137, 2653–2657.

Cattin, A.L., Burden, J.J., Van Emmenis, L., Mackenzie, F.E., Hoving, J.J., Garcia Calavia, N., Guo, Y., McLaughlin, M., Rosenberg, L.H., Quereda, V., et al., 2015. Macrophage-induced blood vessels guide schwann cell-mediated regeneration of peripheral nerves. Cell 162, 1127–1139.

Chanas-Sacre, G., Rogister, B., Moonen, G., Leprince, P., 2000. Radial glia phenotype: origin, regulation, and transdifferentiation. J. Neurosci. Res. 61, 357–363.

Doetsch, F., Garcia-Verdugo, J.M., Alvarez-Buylla, A., 1997. Cellular composition and three-dimensional organization of the subventricular germinal zone in the adult mammalian brain. J. Neurosci. 17, 5046–5061.

Emsley, J.G., Hagg, T., 2003. alpha6beta1 integrin directs migration of neuronal precursors in adult mouse forebrain. Exp. Neurol. 183, 273–285.

Farin, A., Suzuki, S.O., Weiker, M., Goldman, J.E., Bruce, J.N., Canoll, P., 2006. Transplanted glioma cells migrate and proliferate on host brain vasculature: a dynamic analysis. Glia 53, 799–808.

Gong, S., Zheng, C., Doughty, M.L., Losos, K., Didkovsky, N., Schambra, U.B., Nowak, N.J., Joyner, A., Leblanc, G., Hatten, M.E., et al., 2003. A gene expression atlas of the central nervous system based on bacterial artificial chromosomes. Nature 425, 917–925.

Grade, S., Weng, Y.C., Snapyan, M., Kriz, J., Malva, J.O., Saghatelyan, A., 2013. Brain-derived neurotrophic factor promotes vasculature-associated migration of neuronal precursors toward the ischemic striatum. PLoS One 8, e55039.

Hallmann, R., Horn, N., Selg, M., Wendler, O., Pausch, F., Sorokin, L.M., 2005. Expression and function of laminins in the embryonic and mature vasculature. Physiol. Rev. 85, 979–1000.

Hara, H., Huang, P.L., Panahian, N., Fishman, M.C., Moskowitz, M.A., 1996. Reduced brain edema and infarction volume in mice lacking the neuronal isoform of nitric oxide synthase after transient MCA occlusion. J. Cereb. Blood Flow Metab. 16, 605–611.

Holmes, T.C., de Lacalle, S., Su, X., Liu, G., Rich, A., Zhang, S., 2000. Extensive neurite outgrowth and active synapse formation on self-assembling peptide scaffolds. Proc. Natl. Acad. Sci. U. S. A. 97, 6728–6733.
Huttenlocher, A., Horwitz, A.R., 2011. Integrins in cell migration. Cold Spring Harb. Perspect. Biol. 3, a005074.
Ihrie, R.A., Alvarez-Buylla, A., 2011. Lake-front property: a unique germinal niche by the lateral ventricles of the adult brain. Neuron 70, 674–686.
Jin, K., Wang, X., Xie, L., Mao, X.O., Zhu, W., Wang, Y., Shen, J., Mao, Y., Banwait, S., Greenberg, D.A., 2006. Evidence for stroke-induced neurogenesis in the human brain. Proc. Natl. Acad. Sci. U. S. A. 103, 13198–13202.
Kaneko, N., Marin, O., Koike, M., Hirota, Y., Uchiyama, Y., Wu, J.Y., Lu, Q., Tessier-Lavigne, M., Alvarez-Buylla, A., Okano, H., et al., 2010. Neuroblasts clear the path of astrocytic processes for their rapid migration in the adult brain. Neuron 67, 213–223.
Kawauchi, T., Sekine, K., Shikanai, M., Chihama, K., Tomita, K., Kubo, K., Nakajima, K., Nabeshima, Y., Hoshino, M., 2010. Rab GTPases-dependent endocytic pathways regulate neuronal migration and maturation through N-cadherin trafficking. Neuron 67, 588–602.
Kojima, T., Hirota, Y., Ema, M., Takahashi, S., Miyoshi, I., Okano, H., Sawamoto, K., 2010. Subventricular zone-derived neural progenitor cells migrate along a blood vessel scaffold toward the post-stroke striatum. Stem Cells 28, 545–554.
Kokovay, E., Wang, Y., Kusek, G., Wurster, R., Lederman, P., Lowry, N., Shen, Q., Temple, S., 2012. VCAM1 is essential to maintain the structure of the SVZ niche and acts as an environmental sensor to regulate SVZ lineage progression. Cell Stem Cell 11, 220–230.
Ley, K., Rivera-Nieves, J., Sandborn, W.J., Shattil, S., 2016. Integrin-based therapeutics: biological basis, clinical use and new drugs. Nat. Rev. Drug Discov. 15, 173–183.
Li, Y., Song, Y., Zhao, L., Gaidosh, G., Laties, A.M., Wen, R., 2008. Direct labeling and visualization of blood vessels with lipophilic carbocyanine dye DiI. Nat. Protoc. 3, 1703–1708.
Lindvall, O., Kokaia, Z., 2015. Neurogenesis following Stroke Affecting the Adult Brain. Cold Spring Harb. Perspect. Biol. 7.
Lugassy, C., Barnhill, R.L., 2007. Angiotropic melanoma and extravascular migratory metastasis: a review. Adv. Anat. Pathol. 14, 195–201.
Macas, J., Nern, C., Plate, K.H., Momma, S., 2006. Increased generation of neuronal progenitors after ischemic injury in the aged adult human forebrain. J. Neurosci. 26, 13114–13119.
Madisen, L., Zwingman, T.A., Sunkin, S.M., Oh, S.W., Zariwala, H.A., Gu, H., Ng, L.L., Palmiter, R.D., Hawrylycz, M.J., Jones, A.R., et al., 2010. A robust and high-throughput Cre reporting and characterization system for the whole mouse brain. Nat. Neurosci. 13, 133–140.
Marti-Fabregas, J., Romaguera-Ros, M., Gomez-Pinedo, U., Martinez-Ramirez, S., Jimenez-Xarrie, E., Marin, R., Martí-Vilalta, J.L., Garcia-Verdugo, J.M., 2010. Proliferation in the human ipsilateral subventricular zone after ischemic stroke. Neurology 74, 357–365.
Minger, S.L., Ekonomou, A., Carta, E.M., Chinoy, A., Perry, R.H., Ballard, C.G., 2007. Endogenous neurogenesis in the human brain following cerebral infarction. Regen. Med. 2, 69–74.
Mirzadeh, Z., Merkle, F.T., Soriano-Navarro, M., Garcia-Verdugo, J.M., Alvarez-Buylla, A., 2008. Neural stem cells confer unique pinwheel architecture to the ventricular surface in neurogenic regions of the adult brain. Cell Stem Cell 3, 265–278.
Mui, K.L., Chen, C.S., Assoian, R.K., 2016. The mechanical regulation of integrin-cadherin crosstalk organizes cells, signaling and forces. J. Cell Sci. 129, 1093–1100.
Ohab, J.J., Fleming, S., Blesch, A., Carmichael, S.T., 2006. A neurovascular niche for neurogenesis after stroke. J. Neurosci. 26, 13007–13016.
Potocnik, A.J., Brakebusch, C., Fassler, R., 2000. Fetal and adult hematopoietic stem cells require beta1 integrin function for colonizing fetal liver, spleen, and bone marrow. Immunity 12, 653–663.
Schaar, B.T., McConnell, S.K., 2005. Cytoskeletal coordination during neuronal migration. Proc. Natl. Acad. Sci. U. S. A. 102, 13652–13657.
Shen, Q., Wang, Y., Kokovay, E., Lin, G., Chuang, S.M., Goderie, S.K., Roysam, B., Temple, S., 2008. Adult SVZ stem cells lie in a vascular niche: a quantitative analysis of niche cell-cell interactions. Cell Stem Cell 3, 289–300.
Sixt, M., Engelhardt, B., Pausch, F., Hallmann, R., Wendler, O., Sorokin, L.M., 2001. Endothelial cell laminin isoforms, laminins 8 and 10, play decisive roles in T cell recruitment across the blood-brain barrier in experimental autoimmune encephalomyelitis. J. Cell Biol. 153, 933–946.
Snapyan, M., Lemasson, M., Brill, M.S., Blais, M., Massouh, M., Ninkovic, J., Gravel, C., Berthod, F., Gotz, M., Barker, P.A., et al., 2009. Vasculature guides migrating neuronal precursors in the adult mammalian forebrain via brain-derived neurotrophic factor signaling. J. Neurosci. 29, 4172–4188.
Takase, Y., Tadokoro, R., Takahashi, Y., 2013. Low cost labeling with highlighter ink efficiently visualizes developing blood vessels in avian and mouse embryos. Develop. Growth Differ. 55, 792–801.
Tavazoie, M., Van der Veken, L., Silva-Vargas, V., Louissaint, M., Colonna, L., Zaidi, B., Garcia-Verdugo, J.M., Doetsch, F., 2008. A specialized vascular niche for adult neural stem cells. Cell Stem Cell 3, 279–288.
Tronche, F., Kellendonk, C., Kretz, O., Gass, P., Anlag, K., Orban, P.C., Bock, R., Klein, R., Schutz, G., 1999. Disruption of the glucocorticoid receptor gene in the nervous system results in reduced anxiety. Nat. Genet. 23, 99–103.
Tsai, H.H., Niu, J., Munji, R., Davalos, D., Chang, J., Zhang, H., Tien, A.C., Kuo, C.J., Chan, J.R., Daneman, R., et al., 2016. Oligodendrocyte precursors migrate along vasculature in the developing nervous system. Science 351, 379–384.
Wang, X., Qiu, R., Tsark, W., Lu, Q., 2007. Rapid promoter analysis in developing mouse brain and genetic labeling of young neurons by doublecortin-DsRed-express. J. Neurosci. Res. 85, 3567–3573.
Whitman, M.C., Fan, W., Rela, L., Rodriguez-Gil, D.J., Greer, C.A., 2009. Blood vessels form a migratory scaffold in the rostral migratory stream. J. Comp. Neurol. 516, 94–104.
Wichterle, H., Garcia-Verdugo, J.M., Alvarez-Buylla, A., 1997. Direct evidence for homotypic, glia-independent neuronal migration. Neuron 18, 779–791.
Won, C., Lin, Z., Kumar, T.P., Li, S., Ding, L., Elkhal, A., Szabo, G., Vasudevan, A., 2013. Autonomous vascular networks synchronize GABA neuron migration in the embryonic forebrain. Nat. Commun. 4, 2149.
Wu, X., Reddy, D.S., 2012. Integrins as receptor targets for neurological disorders. Pharmacol. Ther. 134, 68–81.
Yamashita, T., Ninomiya, M., Hernandez Acosta, P., Garcia-Verdugo, J.M., Sunabori, T., Sakaguchi, M., Adachi, K., Kojima, T., Hirota, Y., Kawase, T., et al., 2006. Subventricular zone-derived neuroblasts migrate and differentiate into mature neurons in the post-stroke adult striatum. J. Neurosci. 26, 6627–6636.
Zhang, R.L., Chopp, M., Gregg, S.R., Toh, Y., Roberts, C., Letourneau, Y., Buller, B., Jia, L., P Nejad Davarani, S., Zhang, Z.G., 2009. Patterns and dynamics of subventricular zone neuroblast migration in the ischemic striatum of the adult mouse. J. Cereb. Blood Flow Metab. 29, 1240–1250.
Zhang, R.L., Chopp, M., Roberts, C., Liu, X., Wei, M., Nejad-Davarani, S.P., Wang, X., Zhang, Z.G., 2014. Stroke increases neural stem cells and angiogenesis in the neurogenic niche of the adult mouse. PLoS One 9, e113972.